

Sensors and Algorithm Evaluation for Tripwire Detection in the Landmine Detection 4.0 Project

1 st Jonathon Sinton <i>Dept. Of Physics and Astronomy Franklin & Marshall College Lancaster, PA, USA jsinton@fandm.edu</i>	2 nd Timothy D. Bechtel <i>Dept. of Earth and Environment Franklin & Marshall College Lancaster, PA, USA tbechtel@fandm.edu</i>	3 rd Fronefield Crawford <i>Dept. of Physics and Astronomy Franklin & Marshall College Lancaster, PA, USA fcrawfor@fandm.edu</i>	4 th Luca Bossi <i>DINFO University of Florence Florence, Italy l.bossi@unifi.it</i>
5 th Lorenzo Capineri <i>DINFO University of Florence Florence, Italy lorenzo.capineri@unifi.it</i>	6 th Pierluigi Falorni <i>DINFO University of Florence Florence, Italy p.falorni@gmail.com</i>	7 th Gabriella Sallai <i>Dept. of Physics and Astronomy Franklin & Marshall College Lancaster, PA, USA gsallai@fandm.edu</i>	8 th Anastasia Kuske <i>Dept. of Physics and Astronomy Franklin & Marshall College Lancaster, PA, USA akuske@fandm.edu</i>

Abstract—This paper covers advances made in the tripwire detection aspect of the Landmine Detection 4.0 project. This includes algorithmic improvements - most importantly a comparison between a gradient-sigmoid filter and a derivative subtraction filter - and testing of these algorithms on tripwire scenes. We used a Canon DSLR camera for testing, which provides higher resolution and a different spectral range than the FLIR thermal camera we had used in previous testing. We have also begun investigating the use of near-infrared cameras as a possible alternative. Additionally, we have investigated methods to reduce false-positive detections within images with the intention to implement and test some of these methods in the near future.

I. INTRODUCTION

This paper describes progress on tripwire detection within the Landmine Detection 4.0 project [1]. This project aims to develop a multi-sensor robotic system for the semi-autonomous detection of landmines. Sensors include a ground penetrating radar (GPR) and a holographic subsurface radar (HSR) for the detection of buried mines, and a tripwire sensor for the detection of side-attack and directional landmines. The GPR and HSR are currently integrated with the robot via ROS, and the tripwire detector will be implemented in the same manner once it has been further developed.

In this paper, we first describe the motivation for tripwire detection and the current state of the art. We then describe our investigation into image processing algorithms and the testing of these algorithms using a Canon EOS Rebel T5 camera. We then focus on additional improvements to our algorithm that we plan to implement. Finally, we mention the appeal of near infrared cameras and possible cameras to test in our future work.

II. MOTIVATION AND STATE OF THE ART

Contrary to popular perception, buried antipersonnel mines do not provide the only hazard in abandoned minefields. Tripwire and breakwire-triggered fragmentation mines also provide

a significant hazard to both humans and robots attempting to clear these fields. These wires can be made from either metals or dielectric materials and are typically less than a millimeter in diameter [2] (and can even be less than a half-millimeter [3]), which renders them extremely difficult to see with the naked eye. Additionally, the presence of vegetation further obscures these wires.

Previous research on tripwire detection has focused on both image processing techniques to identify tripwires as well as investigations into imagery taken in different spectra. While electromagnetic induction and radar-based methods show promise [2] [4], these are suitable only for metallic tripwires. From our work with authorities in the Donbass conflict zone of Eastern Ukraine, we know that tripwires found there are typically dielectric fishing wire, which renders a technique that only identifies metallic wires insufficient. An acoustic detection method has also been proposed [5], yet issues regarding coupling acoustic energy to a tripwire at a distance make its utility in the field questionable. Numerous studies into the optical detection of tripwires have yielded promising results [6] [7] [8] [9], though none have resulted in a field-ready device. These studies have focused on imagery in the visible, near infrared (NIR), or short wave infrared (SWIR) regimes. Imagery in the NIR and SWIR spectra relies on the contrasting reflectivities of tripwire materials and vegetation.

Nearly all groups that have used imagery to detect tripwires employed the Hough transform to detect straight lines. Only one group used another method – the Radon transform [8]. For simplicity, all of these groups made the assumption that a tripwire would be a straight, roughly-horizontal line. The image processing employed prior to executing the Hough (or Radon) transform varied among these groups. One group attempted to track Hough peaks through image sequences instead of analyzing individual images [7]. If peaks corresponded to lines that were in extremely different image locations throughout a sequence, the signal was categorized as a false alarm. That

same group also created an algorithm to extract horizontal lines from images using a vertical derivative on the image [9]. The Radon transform group used polarized SWIR images and a Sobel edge detection [8]. Another group performed image normalization and vertical differentiation prior to performing a Hough transform [6].

In all of these cases, regardless of the type of image processing or transform employed, the findings did not present more than only preliminary results, and none of the studies could make conclusive claims about the efficacy of the techniques used.

III. ALGORITHMIC INVESTIGATION

The key focus of our algorithmic investigation centered on image processing techniques to employ prior to the Hough transform. We desired a technique to remove as much clutter from the image as possible and/or enhance the signature of the tripwire within the image. This would enable the Hough transform to correctly identify the tripwire at a higher rate.

While our initial algorithm only employed a Canny edge detection followed by the Hough transform [1] (Fig. 1a), we found experimentally that we could increase our detection rate by switching to a derivative subtraction (DS) algorithm. This processed the images by subtracting the second image derivative in the y-direction of the image's pixel values from the first y-derivative (see the defined y-direction in Fig. 2). The use of y-derivatives assumes that the tripwire will be roughly horizontal across the image. We can express the output of this filter (D) as

$$D = \frac{\partial I}{\partial y} - \frac{\partial^2 I}{\partial y^2}, \quad (1)$$

where I is the image. We then performed a Canny edge detection on D , followed by the Hough transform (Fig. 1b).

It is important to note that we came across this DS method through an experimental, iterative process. Thus, this was not

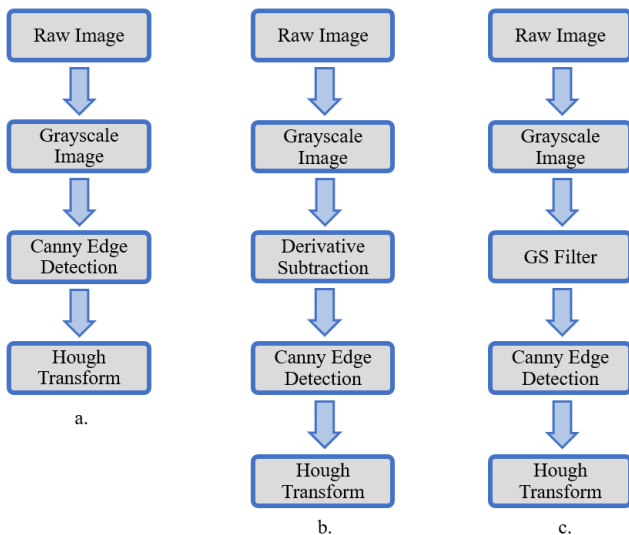


Fig. 1. (a) The original “only edge detection” algorithm. (b) The algorithm that employed the DS filter. (c) The algorithm with the GS filter.



Fig. 2. Image of a sample tripwire scene. Note the definitions of the x and y-directions in the image.

a theoretically proven algorithm. However, we can perform a basic theoretical analysis of this method as it applies to tripwires. In images, an extremely thin, horizontal feature has cross sectional pixel values that roughly resemble a Gaussian function (Figs. 3a and 3b). Subtracting the Gaussian's second derivative from the first derivative amplifies the peak while yielding troughs on either side (Fig. 3c). In an image, this would amplify the center of the tripwire while decreasing pixel values on either side of the tripwire (Fig. 3d). Theoretically, this should enhance the tripwire's visibility to an edge detector. A more in-depth theoretical analysis of this algorithm is beyond the scope of this paper.

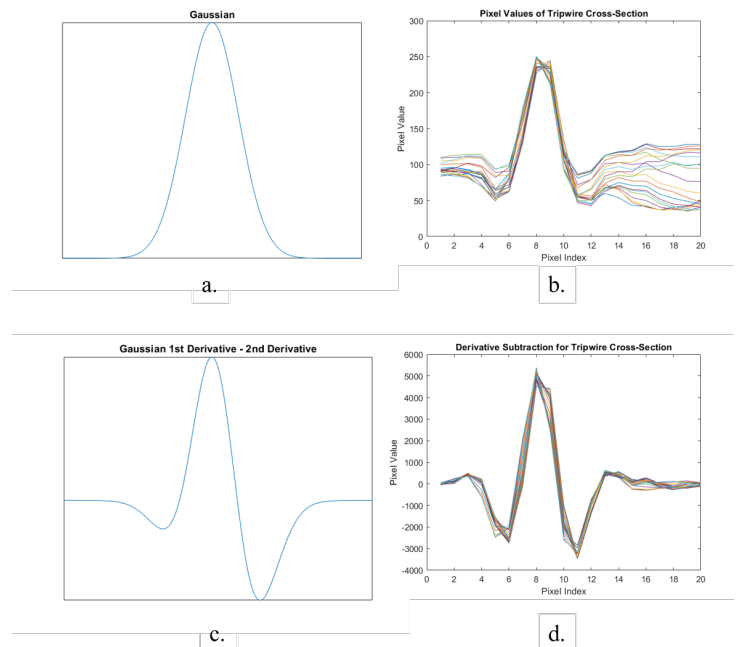


Fig. 3. (a) A Gaussian function. (b) 20 cross sections of a tripwire, in pixel values. (c) The first derivative of a Gaussian minus the second derivative. (d) The first derivative minus the second derivative for the tripwire cross sections.

Since the DS filter was determined experimentally, we opted to compare it to the theoretically demonstrated Gradient Sigmoid (GS) filter [10]. The GS algorithm is the same as the DS algorithm, except it uses a gradient sigmoid filter in place of the derivative subtraction filter (Fig. 1c).

The GS filter functions by processing a grayscale image (\mathbf{I}) and then performing a convolution of the processed image (\mathbf{A}) and a kernel (\mathbf{Q}). We can define the kernel \mathbf{Q} as a column vector of length $2L + 1$ where the first L values equal -1 , the next value equals 0 , and the final L values equal 1 . The value for L should be half of the desired pixel resolution of the tripwire. Since we desire to resolve a tripwire to a width of four pixels, we used $L = 2$ so that the kernel \mathbf{Q} was

$$\mathbf{Q} = \begin{bmatrix} -1 \\ -1 \\ 0 \\ 1 \\ 1 \end{bmatrix}. \quad (2)$$

We can define the processed image as a matrix \mathbf{A} of -1 , 0 , and 1 's:

$$\mathbf{A} = \text{sgn} \left[\frac{\partial \mathbf{I}}{\partial y} \right]. \quad (3)$$

Like with the DS filter, in this case we have assumed that tripwires will be roughly horizontal, and thus the filter only uses a y -derivative. The output of the GS filter (\mathbf{G}) is the convolution

$$\mathbf{G} = \mathbf{A} * \mathbf{Q}. \quad (4)$$

The Canny edge detection was applied after the GS filter since it provided improved detection rates when applying the final Hough transform.

IV. EXPERIMENTAL DESIGN AND TESTING

We tested these algorithms using 42 images of tripwires taken with a Canon EOS Rebel T5 camera and with 308 images previously taken with a FLIR C3 thermal camera. For tripwires, we used nylon fishing lines, since tripwires within the Donbass conflict zone are typically made from fishing line. The images with the Canon camera used wires with diameters of 0.308, 0.437, and 0.493 mm, and the images with the FLIR camera used these and additional wires with diameters of 0.371, 0.526, and 0.587 mm.

We took 14 images of each diameter wire. For each diameter, we took two sets of seven images, where the camera's distance to the wire ranged from 0.50 m to 2.00 m at 0.25 m intervals. For one set of seven images, we placed the wire in front of high-grass vegetation, while for the other set we hid the wire 30 cm within the vegetation.

The images with the Canon camera were all taken in one location, while the images with the FLIR camera had been taken across four locations (all wire diameters were used in all locations, except the 0.526 mm wire, which was only used in two locations).

The Canon EOS Rebel T5 camera is a visible-light spectrum camera with a resolution of 5184×3456 pixels. The camera

provides raw image files in the Canon raw image format (with a filename extension `.cr2`). This meets our requirement of using raw images for tripwire detection, and it nearly meets the resolution requirement for resolving a 0.5 mm diameter tripwire to four full pixels (the requirement is 5728×4328 pixels; see Appendix A for this derivation).

The FLIR C3 thermal camera combines far infrared and visible light imagery through the camera's "Thermal MSX" feature. It has a resolution of only 320×240 , and it only stores compressed JPEG images. While the quality of these images is far below the Canon's quality, these images remained from our investigation of the use of thermal imagery [1], and they provided a large sample size to test the various algorithms.

V. EXPERIMENTAL DATA AND ANALYSIS

Tripwire detection rates for the various algorithms applied to both the Canon and FLIR images are listed in Table I. As noted above, we compared the DS algorithm to the GS algorithm that employed a Canny edge detection. This is because we determined a significantly higher detection rate for the GS filter when the edge detection was also employed. We did not test the FLIR images with the GS filter without the edge detection because of this determination.

These results indicate that the DS algorithm achieves a significantly better detection rate than the GS filter algorithm. Additionally, the DS algorithm achieved a significantly higher rate (p value of 0.0396) among the FLIR images than the algorithm with only edge detection. While the results for the DS algorithm and the algorithm with only edge detection were not significantly different for the Canon images, this is most likely due to the fact that the "only edge detection" algorithm achieved such a high detection rate. Any improvements on a detection rate in the 90th percentile would naturally have diminishing returns. However, before determining that the DS algorithm improvement is unnecessary for high resolution images, it is important to remember that the Canon images are from only one location.

Most importantly, the theoretically supported GS filter algorithm achieved significantly lower detection rates than both the DS algorithm and the algorithm with only edge detection. Not only does the DS algorithm appear to be the better algorithm for detecting tripwires, but this also raises questions about the efficacy of the GS algorithm for detecting thin linear components in highly cluttered images.

TABLE I
DETECTION RATES (%) FOR THE DIFFERENT ALGORITHMS WITH THE
CANON AND FLIR CAMERAS

	Only Canny Edge Detection	DS Filter (with edge detection)	GS Filter (with edge detection)	GS Filter (no edge detection)
Canon	95.2	97.6	81.0	59.5
FLIR	32.8	39.6	24.3	N/A

One unexpected result was that the thickest wire provided the lowest detection rate in the Canon images. In both the "only edge detection" and DS filter algorithms, the failed

detections only occurred with the thickest wire, and the GS filter algorithm yielded a 64.3% detection rate with the thickest wire while the thinnest wire provided a 100% detection rate. However, with only 14 images per wire diameter, we cannot draw any significant conclusions about the effect of the wire width. One factor that may have influenced these results was that the images of the thicker wires were taken later in the afternoon than those of the thinner wires, which caused slightly different lighting conditions. Such variance in ambient conditions may be a factor to consider.

VI. FUTURE ALGORITHMIC IMPROVEMENTS

While the DS filter appears to successfully raise the detection rate by emphasizing thin linear features within images, further improvements can be made to the algorithm. The aim of the algorithm is to detect a tripwire by identifying the maximum value within the Hough transform space. Since local maxima within the space correspond to straight lines, the absolute maximum within the space ideally corresponds to the tripwire. However, we have seen that this is not always the case. Occasionally, that maximum corresponds to other linear features, such as the line between the image's foreground and background, or extremely long, straight pieces of vegetation. Occasionally, when the tripwire is extremely well obscured, the Hough maximum may correspond to seemingly random features within the image. We can employ image segmentation procedures to remove false positives caused by non-tripwire objects, and we can employ a series of images to remove those caused by seemingly random features.

Such varying causes of false positives require various methods to reject those maxima so that the next highest maximum within the transform is recognized. For rejecting linear plants (such as grasses), we have found that these plants appear after the Canny edge detection as two approximately parallel lines. We have found that the tripwires also appear as parallel lines, yet these lines are much closer together in pixel distance. Thus, a method for rejecting lines from grasses and other linear plant features would be to reject a Hough peak if there exists another peak that corresponds to a nearby parallel line beyond a certain pixel distance away.

False positives that are caused by peaks corresponding to the line between the foreground and background (or other areas) within an image can be rejected by comparing the pixel values above and below the line. The pixel values directly above and below a tripwire should be nearly equal because a tripwire is a single image segment layered on top of another single image segment. Therefore, the pixel values above and below a tripwire should have similar values because they correspond to a single segment. Additionally, a tripwire is so thin that there should not be a major change in pixel value across the hidden portion of the segment behind the wire. However, the pixels above the line delineating a foreground from a background (for example, a horizon line) should have significantly different values from the pixels below. This is due to the fact that this line separates two distinct image segments.

Another source of false positives occurs when the maximum in the Hough transform corresponds to seemingly random features in the image. This problem was briefly addressed by a group at the University of Missouri and the University of Florida in 2004 [7]. This group analyzed sequences of images taken as a robot progressed through a mine field. Their algorithm would then compare detected lines from sequential images, and if the lines were at extremely different angles or in extremely different locations within the image, their algorithm would reject those lines. They consistently found a higher detection accuracy when analyzing image sequences than when analyzing individual images. We could use a similar technique in order to remove false positives due to seemingly random features. However, this would also necessitate that we change our algorithm from analyzing a single image to analyzing an image sequence. Therefore, we would first need to implement the previous two adjustments (to reject false positives from linear plants and lines between different image areas) and then determine whether implementing an image sequence analysis would be a necessary or useful change.

VII. INVESTIGATION INTO NEAR-INFRARED CAMERAS

While our Canon EOS Rebel T5 has been a dramatic improvement over the FLIR thermal camera that we previously used, literature has shown that the greatest difference in reflectivity between tripwire materials and vegetation occurs in the near-infrared (NIR) spectrum in the 700-1300 nm range [6]. However, in our tests with a cheap, off-the-shelf infrared camera having an estimated spectral range of 700-800 nm, none of our algorithms could detect a single tripwire. We believe that three factors could have influenced these non-detection rates. The first is that this is a very low-cost off-the-shelf camera designed to function as a night-vision security camera. As such, the camera has a fish-eye effect, which affects the geometry of the images. This is crucial because our algorithm attempts to detect straight lines. Second, since the camera was not designed for scientific purposes, we cannot determine exactly where on the NIR spectrum the camera is most effective. Research into similar security cameras shows that it is most likely viewing the 700-800 nm range, but it is unclear how effectively the camera actually views that range. Third, this camera provided only JPEG images instead of raw images. Thus, information is lost with image compression.

While these basic preliminary tests with a low-quality NIR camera did not appear to support the literature that the NIR spectrum provides the best wavelengths for tripwire detection, we believe that the low-quality of our camera may account for this discrepancy. As such, conducting tests with a high quality NIR camera would be informative. We have looked into several high-quality cameras for this purpose, including the Mini-SWIR 1280JSX High Definition Camera, the IMPERX C5180 camera, and Hamamatsu InGaAs cameras.

VIII. CONCLUSION

Our work suggests innovations in algorithms for automated tripwire detection systems. We have experimentally shown that

our DS filter outperforms both a simple edge detection as well as the theoretically sound GS filter. We believe that the DS filter presents an improvement in enhancing thin, horizontal, linear features in images. However, more work is required to develop the theory as to why this works so effectively.

In addition to further investigating the DS filter, there is still room for improvement within other aspects of our tripwire detection system. Including image segmentation techniques in our algorithm could allow us to reject false alarms that are created by non-tripwire linear features. The analysis of image sequences instead of individual images could reduce false alarms from seemingly random features within the image, as has been previously demonstrated. Finally, the use of NIR images is another very promising avenue that requires further investigation.

APPENDIX A CAMERA RESOLUTION REQUIREMENTS

Ideally, the camera's optics must be able to resolve a tripwire (less than 0.5 mm wide) to a width of at least four pixels from one meter away (Fig. A1). To satisfy this requirement, the camera's resolution can be calculated mathematically, dependent on the field of view (FOV) of the lens. We can express the necessary camera resolution ($m \times n$) as:

$$m \times n = \frac{\alpha}{\theta} \times \frac{\beta}{\theta}, \quad (\text{A.1})$$

where α and β are the lens' FOV in radians and θ is the number of radians per pixel of the tripwire. We can express θ as:

$$\theta = \frac{\arctan(y/x)}{p} \approx \frac{y}{px}, \quad (\text{A.2})$$

where y is the width of the tripwire, x is the distance from the camera to the tripwire, and $y \ll x$ is assumed. Here p is the desired width, in pixels, of the tripwire. Therefore, we find:

$$m \times n = \frac{px}{y}(\alpha \times \beta). \quad (\text{A.3})$$

We desire that the robot initially detects the wire at a distance no closer than 1 meter ($x = 1$), and we set conditions that tripwires are typically < 0.5 mm wide ($y = 0.0005$) and that the desired width of the tripwire is 4 pixels ($p = 4$) in the image. We use a typical camera FOV of $41^\circ \times 31^\circ$ ($\alpha \times \beta = 0.716 \text{ rad} \times 0.541 \text{ rad}$). These stringent requirements yield a minimum camera resolution of 5728×4328 .

APPENDIX B ALGORITHM IMAGES

The images on the following page depict Fig. 2 after undergoing the Canny Edge detection in the DS and GS algorithms. The Hough transform successfully found the tripwire in both images.

ACKNOWLEDGMENT

This work was funded in part by the Howard Patton fund at Franklin and Marshall College and by NATO Science for Peace and Security Programme Project G5014.

REFERENCES

- [1] L. Capineri *et al.*, "Machine vision for obstacle avoidance, tripwire detection, and subsurface radar image correction on a robotic vehicle for the detection and discrimination of landmines," *PIERS Rome*, 2019.
- [2] G. N. Crisp, C. R. Thornhill, and G. Gooding-Williams, "Detection of wires using UWB radar," *Ultra-Wideband, Short-Pulse Electromagnetics*, vol. 6, pp. 471–480, 2003.
- [3] S. K. Babey *et al.*, "Feasibility of optical detection of landmine tripwires," *SPIE Proceedings*, vol. 4038, pp. 220–231, 2000.
- [4] L. J. Carter and L. C. Y. Liao, "An optimal technology for detection of vegetation-obscured tripwires," *SPIE Proceedings*, vol. 6217, 2006.
- [5] L. Carter and C. Y. Liao, "A new approach to detecting vegetation-obscured tripwires," *ICHS 2006 Proceedings*, vol. 1, pp. 619–624, 2006.
- [6] T. H. Allik *et al.*, "Eyesafe laser illuminated tripwire (elit) detector," *SPIE Proceedings*, vol. 4394, pp. 176–186, 2001.
- [7] R. Luke *et al.*, "Experiments in tripwire detection using visible and near IR imagery," *SPIE Proceedings*, vol. 5415, pp. 754–762, 2004.
- [8] D. J. Daniels *et al.*, "Use of COTS technology in tripwire detection," *SPIE Proceedings*, vol. 5415, pp. 734–744, 2004.
- [9] J. M. Keller *et al.*, "Real-time tripwire detection on a robotic testbed," *SPIE Proceedings*, vol. 5089, pp. 1287–1297, 2003.
- [10] L. Capineri, P. Falorni, and C. Windsor, "Buried mine classification from three-dimensional radar data," *Insight - Non-Destructive Testing and Condition Monitoring*, vol. 44, 2002.

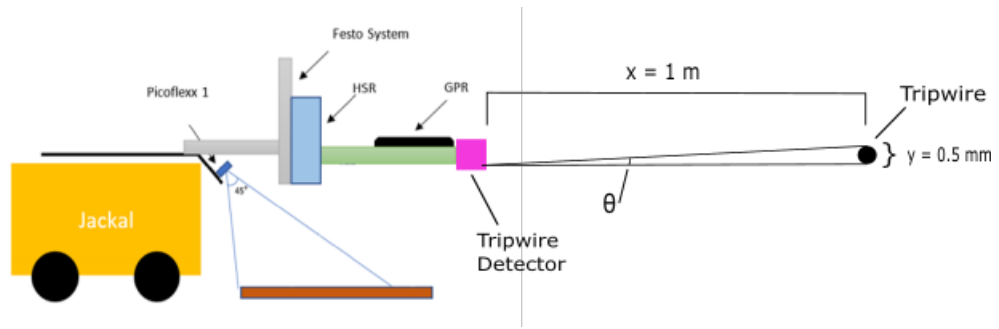


Fig. A1. A depiction of the ideal scenario for the robot detecting a tripwire. The tripwire detector is at a distance of $x = 1$ m from the wire, and the tripwire has a width of $y = 0.5$ mm.

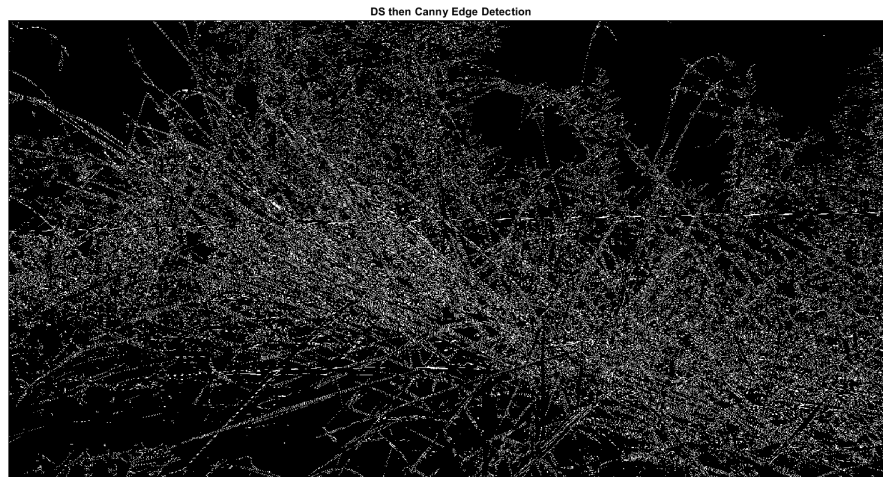


Fig. B1. Edge detection performed on a DS filtered image

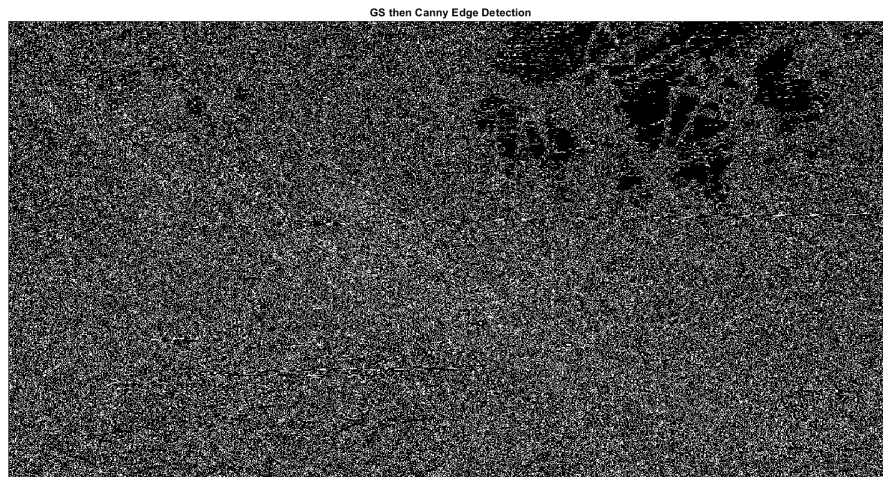


Fig. B2. Edge detection performed on a GS filtered image